Local Conformational Changes in the *Vibrio* Na^+/Galactose Cotransporter†

Marloes Veenstra,‡ Seren Lanza,‡ Bruce A. Hirayama, Eric Turk, and Ernest M. Wright*

Department of Physiology, The David Geffen School of Medicine at UCLA, University of California, Los Angeles, California 90095-1751

Received September 23, 2003; Revised Manuscript Received January 22, 2004

ABSTRACT: Na^+ and sugar transport by cotransporters (symporters) is thought to occur as a series of ordered ligand-induced conformational changes. To localize these conformational changes in a bacterial Na^+/galactose cotransporter, we have employed a combination of cysteine-scanning and fluorescence techniques. Single or pairs of cysteine residues were introduced into the external face of a cysteine-less *Vibrio parahaemolyticus* sodium/glucose cotransporter for expression in *Escherichia coli*, and each transporter was purified using affinity chromatography. All the mutant proteins retained transport activity in bacteria and proteoliposomes. Each mutant was exposed to two different fluorescence reagents, ThioGlo3 or pyrene maleimide, that are essentially nonfluorescent until they react with a thiol. Fluorescence was recorded as a function of time and ligand concentrations. The reagents specifically labeled six of the seven cysteine mutants, but only in Cysteine 423 was the fluorescence affected by ligands. The rate of labeling of Cys423 by ThioGlo3 or pyrene maleimide was reduced by D-galactose in Na^+ buffer. Furthermore, the fluorescence of Thioglo3-labeled Cys423 was quenched by D-galactose, but only in the presence of Na^+. This quench was not accompanied by a Stokes shift and was not produced by nontransported sugars, e.g., L-glucose. Reducing the sodium concentration from 200 to 10 mM decreased the apparent affinity for D-galactose without altering the maximum quench with saturating D-galactose. Reducing the galactose concentration from 20 to 0.5 mM reduced both the apparent affinity for Na^+ and the maximum quench at saturating Na^+. These results suggest an ordered reaction scheme with Na^+ binding first. The fluorescence results with ThioGlo3-labeled Cys423 indicate that conformational changes underlying Na^+/galactose cotransport occur at or near the extracellular domain between transmembrane helices 10 and 11.

The *Vibrio parahaemolyticus* Na^+/galactose cotransporter is a member of the large SGLT[1] family (*1*, *2*). We have a long-standing interest in mammalian Na^+/sugar cotransporters and have initiated studies of this bacterial orthologue to unravel the relationships between the structure and function of these molecular machines. So far, we have reported success in the overexpression and purification of functional vSGLT protein for electron microscopic, ATR-FTIR, and fluorescence experiments, as well as chemical cross-linking (*3*−*6*). These have demonstrated that vSGLT functions as a monomer and that the transport cycle involves conformational changes in the protein, a feature in common with the mammalian Na^+/sugar cotransporters (*7*−*10*). The ATR-FTIR study revealed a stepwise increase in helicity of the protein upon the addition of sodium and then galactose, which was accompanied by a stepwise reduction in hydrogen/deuterium exchange rates. These results suggest that the equivalent of 52 residues in the 558-amino acid protein are involved in the molecular rearrangements underlying Na^+/D-galactose transport.

To localize these vSGLT conformational changes, we have conducted cysteine-scanning experiments using fluorescence probes. The approach was to introduce cysteine residues into the external face of the cysteine-less protein, expose the reconstituted protein to fluorescent maleimides, and record fluorescence changes of the labeled transporter in the presence and in the absence of ligands. The fluorescence measurements included rates of labeling, spectra, and fluorescence resonance energy transfer (FRET) from native tryptophans. The results show a Na^+-dependent, D-galactose-specific effect on the fluorescence of probes attached to Cys423 on the hydrophilic loop between transmembrane helices (TMHs) 10 and 11, and not at five other locations. These results are consistent with conformational studies of human SGLT1 and lend support to our hypothesis that sugar translocation through SGLT occurs within a domain bounded by TMHs 10−14 (*9*−*13*).

EXPERIMENTAL PROCEDURES

Materials and Methods. D-Galactose, L-glucose, L-arabinose, and cholesterol were purchased from Sigma (St. Louis, MO), and decyl-β-D-maltoside and dodecyl-β-D-maltoside were from Anatrace (Maumee, OH). Asolectin (unfractionated soy phopholipids) was obtained from Associated Concentrates (Woodside, NY), 2-aminoethylmethanethiosulfonate (MTSEA) and sodium (2-sulfonatoethyl)methane-

† This work was supported by a grant from the NIH (DK 44602).

‡ These authors contributed equally to this study.

* To whom correspondence should be addressed. Tel.: (310) 825-6905. Fax: (310) 206-5886. E-mail: ewright@mednet.ucla.edu. www.physiology.ucla.edu/wrightlab

[1] Abbreviations: vSGLT, *Vibrio parahaemolyticus* sodium/glucose cotransporter; $K_{0.5}$, apparent affinity; TMH, transmembrane helix; ATR-FTIR, attenuated total reflection Fourier transform infrared spectroscopy; MTSEA, (2-aminoethyl)methanethiosulfonate; MTSES, sodium (2-sulfonatoethyl)methanethiosulfonate; MIANS, 2-(4′-maleimidylanilino)naphthalene-6-sulfonic acid; IAEDANS, 5-((((2-iodoacetyl)amino)ethyl)amino)naphthalene-1-sulfonic acid; TCEP, tris(2-carboxyethyl)phosphine hydrochloride; ThioGlo3, 9-acetoxy-2-(4-(2,5-dihydro-2,5-dioxo-1*H*-pyrrol-1-yl)phenyl)-3-oxo-3*H*-naphtho[2,1-*b*]pyran.

10.1021/bi0357210 CCC: $27.50
Published on Web 03/02/2004

thiosulfonate (MTSES) from Toronto Research Chemicals Inc. (Ontario, Canada), ThioGlo3 from Covalent Associates (Woburn, MA), and pyrene maleimide, MIANS, IAEDANS, and tris(2-carboxyethyl)phosphine hydrochloride (TCEP) from Molecular Probes (Eugene, OR).

Site-Directed Mutagenesis To Form p3R6A, p3C4, p3C80, p3C149, p3C228, p3C423, p3C477, p3C546, and p3DC1. All studies were carried out with the p3R6 construct, a derivative of the original pVNH6A plasmid, which encodes the fusion construct of *Vibrio* SGLT bearing the native N-terminus and a C-terminal polyhistidine (*3*). It was further mutagenized (*14*) to incorporate the following mutations to result in the construct p3R6A. (a) Silent mutations were made to introduce unique restriction sites between each putative TMH. (b) C411A was made to render this construct cysteine-less. (c) R32K and R522K were introduced for other purposes. (d) The appended C-terminal periplasmic extension was replaced with one encoding a 15th transmembrane span (nearly identical to that of human glycophorin A) and a C-terminal cytoplasmic polyhistidine. The complete C-terminal appendage encodes VNADAEITLIIFGVMAGV-IGTILLISYGIKKLIKASYKSGGSPGHHHHHH, where the 15th transmembrane span is underlined. This Cys-less construct, p3R6A, expressed in intact cells, exhibited 122% the Na-dependent galactose uptake activity of native vSGLT, and about 11−20-fold greater activity than the original VNH6A construct (*3*).

Site-directed mutagenesis of p3R6A produced the following cysteine-containing mutants: p3C4 (I4C), p3C80 (I80C), p3C149 (L149C), p3C228 (A228C), p3C423 (A423C), p3C477 (M477C), p3DC1 (L149C and A423C), and p3C546 (C546). The fidelity of all mutagenized inserts was verified by DNA sequencing.

Expression and Purification. The cysteine-less protein p3R6A, as well as the single-cysteine mutants p3C4, p3C80, p3C149, p3C228, p3C423, p3C477, and p3C546 and a double-cysteine mutant p3DC1 (149C/423C), were expressed in *Escherichia coli* (*3*, *5*). The bacteria were grown overnight at 30 °C after addition of L-arabinose to 6.7 μM to induce protein expression. Cells were pelleted and resuspended in 100 mM NaCl, 100 mM Tris·Cl, pH 8.0, 5 mM Na_3EDTA, and 20% (w/v) sucrose. Hen lysozyme was added to 1 mg/mL, followed by the addition of one volume of water to induce an initial osmotic shock. After 5 min at 22 °C, spheroplasts were cooled on ice to 5−10 °C. Phenylmethylsulfonyl fluoride was added to 0.2 mM, galactose to 20 mM, and NaCl to 100 mM. The spheroplasts were pelleted and then resuspended on ice in 75 mM Tris·Cl, pH 8.0, 200 mM NaCl, 20 mM galactose, 15 mM β-mercaptoethanol, and 5 μg/mL each of RNase A, phenylmethylsulfonyl fluoride, and aprotinin. The suspension was homogenized in a motorized glass/Teflon device, and the membranes were then solubilized with ~0.2% each decyl-β-D-maltoside and dodecyl-β-D-maltoside. Cell debris and DNA were precipitated with 6 mM spermine and pelleted at 27000*g* for 10 min. The supernatant was filtered and applied first to a Ni^{2+} chelate resin and then to a Superose R12 gel filtration column. The purity of the proteins, as determined by Ag^+ staining after SDS−PAGE, was ~90%.

Analytical Methods. Protein concentration was determined by the BCA protein assay (Pierce, Rockford, IL) using bovine serum albumin as a standard. SDS−PAGE (*15*) and Ag^+ staining (*16*, *17*) were done as previously described.

Reconstitution of p3R6A and Cysteine Mutants. Lipids and proteoliposomes were prepared using 90 mg of Asolectin soy lecithin, 10 mg of cholesterol, and 500 μg of purified protein (*3*, *5*). The lipid-to-protein ratio was 7.2:1. The proteoliposome buffer was exchanged with 50 mM potassium phosphate on a 7-mL bed of Superdex 30. The proteoliposomes were pelleted and stored at −80 °C.

Transport Assays. Na^+-dependent D-galactose transport assays of vSGLT (p3R6A) and the cysteine mutants, reconstituted into liposomes, were performed to ensure the proteins were active (*3*, *5*). Transport assays were also carried out on cells expressing the mutants to determine whether sulfhydryl reagents (MTSEA and MTSES) inhibited galactose transport. The cells were incubated for 1 min with 1 mM MTSEA or MTSES prior to the galactose transport assay.

Fluorescence Measurements. The resuspended proteoliposomes underwent four freeze/thaw cycles in liquid nitrogen/37 °C water bath prior to all fluorescence experiments. The fluorescence measurements were initially performed on an Aminco-SLM 4800 spectrofluorometer (Urbana, IL) at a band-pass of 4 nm in a 100-μL nominal volume quartz cuvette, and later on a Fluorolog-3 instrument (Jobin Yvon Horiba, New York, NY).

For the time course of labeling, ThioGlo3, pyrene maleimide, IAEDANS, or MIANS (5−15 μM final concentration) was added to 4 μL of proteoliposomes in 120 μL of 200 mM sodium or potassium phosphate buffer pH 7.0 (*5*). The fluorophores used are essentially nonfluorescent until they are reacted with a thiol. The baseline signal was recorded for 25 s prior to the addition of the probes to the cuvette ($t = 0$). The sugars, 10 mM D-galactose or 10 mM L-glucose, were added either before the fluorescence recording began or after the fluorescence signal had reached a steady state. Control experiments were carried out with liposomes, with proteoliposomes of the Cys-less parent construct (p3R6A), and with the cys-mutants preincubated with MTSEA or another probe, e.g., pyrene maleimide. The $K_{0.5}$ for D-galactose was determined by adding increasing concentrations of D-galactose to ThioGlo3-labeled Cys423 liposomes, and the nontransported sugar L-glucose was used as a control.

Energy-transfer experiments between tryptophan and ThioGlo3 were performed using proteoliposomes in 200 mM potassium phosphate buffer, pH 7.0. The tryptophans were excited at 288 nm, and the emission was recorded from 300 to 480 nm. The spectral data for each energy-transfer experiment were obtained by averaging two to three spectra. ThioGlo3 was added to a final concentration of 5 μM, sodium to 150 mM, and D-galactose or L-glucose to 10 mM. To examine pyrene maleimide excimer formation in the double-cysteine mutant L149C/A423C, the proteoliposomes were incubated with 15 μM pyrene maleimide for 1 h in the dark both with and without the reducing agent TCEP in 200 mM Na^+, 200 mM Na^+ + 10 mM D-galactose, 200 mM K^+, or 200 mM K^+ + 10 mM D-galactose. Pyrene was then excited at 338 nm, and emission spectra were taken from 350 to 500 nm.

All experiments were carried out at 22 °C.

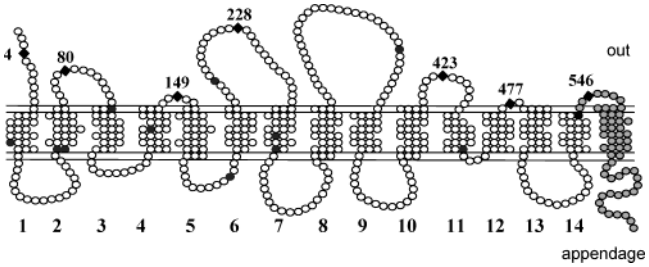

FIGURE 1: Topology of vSGLT. Schematic diagram showing the location of the 7 cysteine residues introduced (◆) and the 12 native tryptophan residues (●) in the cysteine-less vSGLT. The protein consists of 14 transmembrane helices and an appended glycophorin transmembrane helix with a hexa-histidine tail (gray circles). Single cysteine residues were inserted in each of the outer loops between the seven helices that make up the N-terminal half of the protein.

Table 1: D-Galactose Uptakes into VSGLT Proteoliposomes[a]

construct	+ Na^+ (pmol mg^{-1} min^{-1})	− Na^+ (pmol mg^{-1} min^{-1})
Cys-less	164 ± 8	23 ± 4
14C	51 ± 4	9 ± 3
I80C	394 ± 4	31 ± 8
L149C	276 ± 8	65 ± 4
A228C	376 ± 23	21 ± 4
A423C	78 ± 1	13 ± 1
M477C	18 ± 1	3 ± 1
546C	355 ± 49	36 ± 6
L149C/A423C	130 ± 7	49 ± 3

[a] The initial rates of 12 μM [^{14}C]-D-galactose uptakes were measured in triplicate in the presence and in the absence of Na^+. Each cysteine mutant was assayed individually using the cysteine-less vSGLT (p3R6A) and empty liposomes as controls. Uptakes are presented as the mean with the standard deviation. The uptakes into proteoliposomes in the absence of Na^+ were no different than those into empty liposomes.

RESULTS

The location of the 7 introduced cysteines and the 12 native tryptophan residues in vSGLT are shown in Figure 1. The introduced cysteines are located in the external hydrophilic loops, with Cys4 in the N-terminal loop and C80, C149, C228, C423, C477, and C546 between helices. The cysteines were introduced in the outer loops so that they would be readily accessible for labeling by fluorescence probes. It should be noted that the reconstitution of vSGLT into liposomes probably results in only ~50% of the transporters being in the correct orientation, i.e., ~50% with the cysteine(s) facing the outside solution.

All proteins in liposomes were active, showing sodium-dependent D-galactose uptake (Table 1). The D-galactose uptake activity for the least active mutant, M477C, was 10% of the parent construct (p3R6A) in proteoliposomes. In the absence of Na^+, galactose uptakes were similar to those obtained for empty liposomes in the presence and in the absence of Na^+ (not shown). Pretreatment of bacterial cells expressing the mutants with 1 mM MTSEA or MTSES for 1 min did not inhibit D-galactose uptake by either the Cys-less or the I4C mutants (not shown). MTSEA did inhibit D-galactose uptake by I80C (94%), L149C (81%), A288C (50%), A423C (68%), and M477C (40%). MTSES inhibited D-galactose uptake by I80C (80%) and A288C (36%), but L149C and A423C were less sensitive to inhibition by the negatively charged reagent (15% and 25%, respectively). The differential effects of the positively and negatively charged reagents on L149C are similar to those reported previously for the analogous human SGLT1 mutant A166C (*18*).

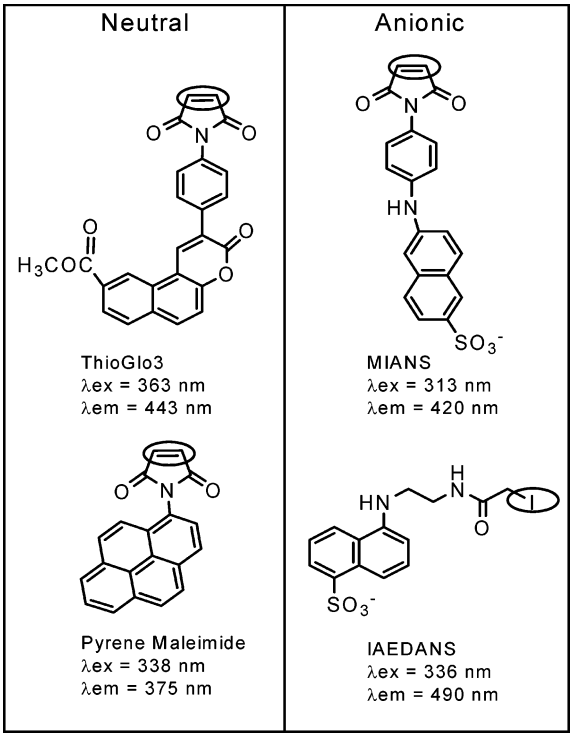

FIGURE 2: Structure and spectral properties of the fluorescence reagents employed in this study.

Fluorescence Experiments. Our strategy was to use specific thiol reagents (Figure 2) which are essentially nonfluorescent until they have reacted with the thiols (*19*, *20*). As controls, we recorded the fluorescence of the reagents incubated with cysteine-less protein (p3R6A) in proteoliposomes and with liposomes. ThioGlo3 was used because of its high quantum yield (0.78 as the glutathione adduct, 0.005 for the reagent), fast reactivity (<1 min in aqueous solutions at 22 °C), and the overlap of its absorbance spectrum with the emission spectrum of tryptophan (*20*). Pyrene maleimide was chosen because its conjugates can form excited-state dimers (excimers) that emit at longer wavelengths than pyrene alone. IAEDANS and MIANS were chosen because their fluorescence is very sensitive to the aqueous solvation state (*19*). MIANS develops appreciable fluorescence when conjugated to thiols in hydrophobic sites. In general, the reagents were added to the cuvette containing proteoliposome suspensions in the presence or in the absence of ligands (Na^+ and D-galactose), and fluorescence was recorded with time. In some experiments, the ligands were added to proteoliposomes in the cuvette after the fluorescence had already approached a steady state.

Examples of the fluorescence labeling time courses are shown in Figure 3. Fluorescence of proteoliposomes in Na^+ buffer was followed upon the addition of 5 μM ThioGlo3. The Cys423 proteoliposomes (Figure 3A) were preincubated for 1 min in Na^+ buffer with or without 1 mM MTSEA. In the absence of MTSEA there was a biphasic increase in ThioGlo3 fluorescence: a predominant fast component, $t_{1/2}$ = 40 s, and a minor slower component, $t_{1/2}$ = 350 s. Pretreatment of the proteoliposomes with MTSEA or MTSET eliminated the fast component. Only the slow ThioGlo3

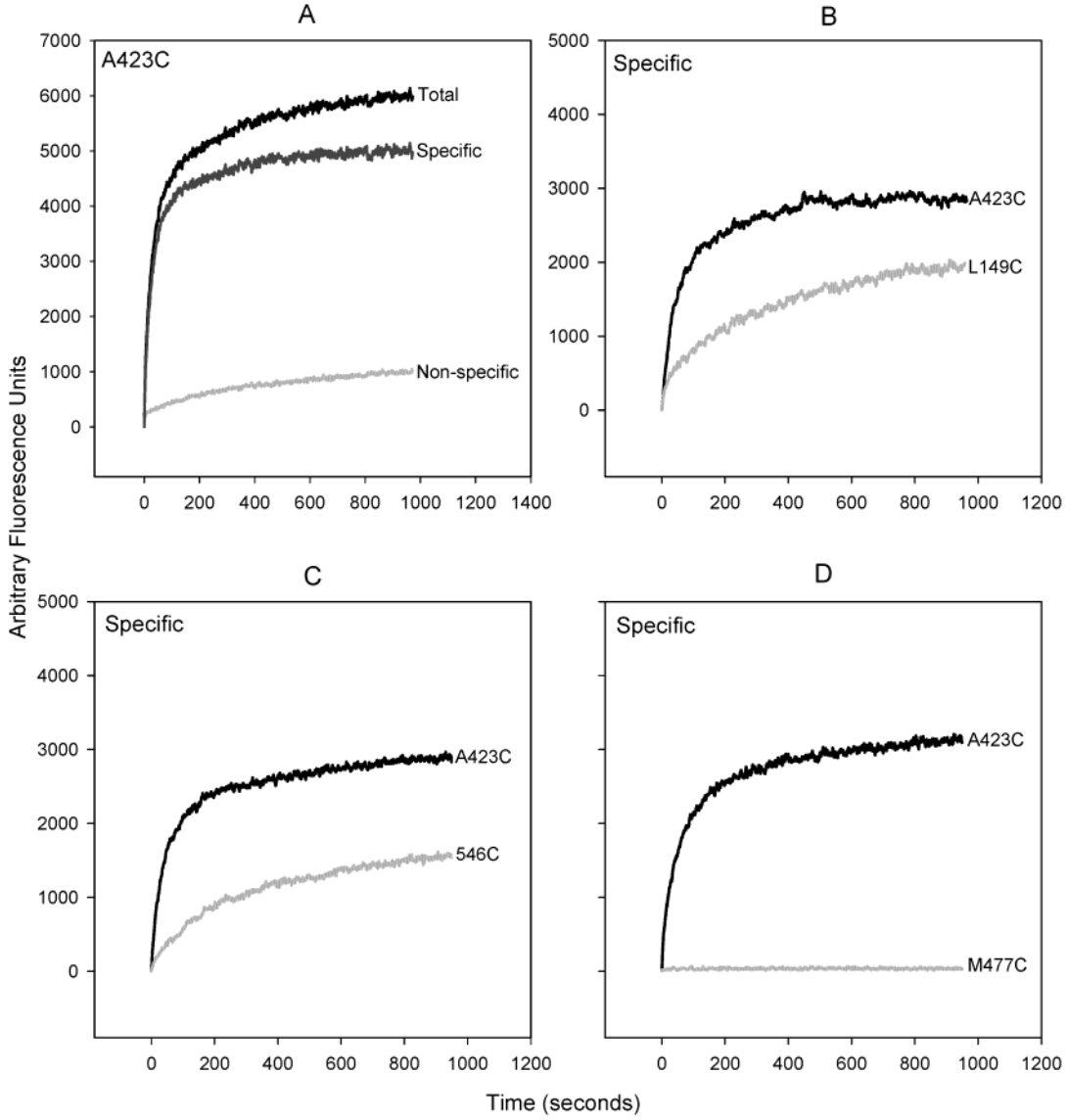

FIGURE 3: (A) Time course of the reaction of ThioGlo3 with Cys423 vSGLT proteoliposomes suspended in 200 mM NaPi buffer at pH 7.0. The fluorescence was recorded at 443 nm upon excitation at 363 nm. After 25 s ($t = 0$), 5 μM ThioGlo3 was added to the cuvette (a 10 s break in the recording) and the fluorescence was recorded (total). Also shown is the fluorescence recorded after preincubation of the proteoliposomes with 1 mM MTSEA for 1 min (nonspecific). This latter signal was comparable to that recorded for liposomes and Cys-less proteoliposomes. The difference between the total and nonspecific fluorescence signals is shown as the specific labeling of Cys423 with ThioGlo3 (specific). (B−D) Paired experiments where Cys149, Cys546, and Cys477 were labeled with ThioGlo3 as described in (A). Each record was corrected for nonspecific labeling by subtracting the fluorescence curve obtained for protein-free liposomes.

component was observed when A423C proteoliposomes were preincubated with pyrene maleimide. A slow component was also recorded with the Cys-less vSGLT1 (p3R6A) or empty liposomes (not shown). These results suggest that the slow component of the ThioGlo3 fluorescence of Cys423 is nonspecific and likely caused by slow partitioning of the dye into the bilayer. The differences between the total fluorescence and this nonspecific component gave the specific fluorescence due to ThioGlo3-derivatized Cys423. The time constant for the reaction of ThioGlo3 with Cys423 ranged from 30 to 60 s. Identical time courses were obtained in K^+ and in choline buffers (not shown). The emission maximum of ThioGlo3 bound to Cys423 was 443 nm, close to that reported in ethanol (*20*).

The rates of specific ThioGlo3 reaction with Cys149 and with Cys546 were slower than those with Cys423, $t_{1/2} = 355$ and 305 s (Figure 3B,C), and Cys477 was completely unreactive (Figure 3D). The time courses for ThioGlo3 labeling of Cys4, Cys80, and Cys228 were comparable to those for Cys423 and Cys149 (not shown), and in each case the peak of the emission spectrum was 443 nm.

The specific pyrene maleimide reaction with Cys423 followed a time course with predominant rapid ($t_{1/2} \approx 50$ s) and minor slow components (Figures 4B). The slow component had a variable magnitude, and this may be due to labeling of Cys423 oriented toward the liposome interior. The emission spectrum of the labeled Cys423 was identical to that for the 2-mercaptoethanol adduct of pyrene maleimide (i.e., emission maximum at 375 nm with a secondary peak at 396 nm). Again, no specific labeling of Cys477 with pyrene was observed, but all the other mutants were labeled.

The anionic dye MIANS was evidently unable to produce a fluorescent signal with either Cys149 or Cys423 in proteoliposomes. Yet MIANS evidently could label these two

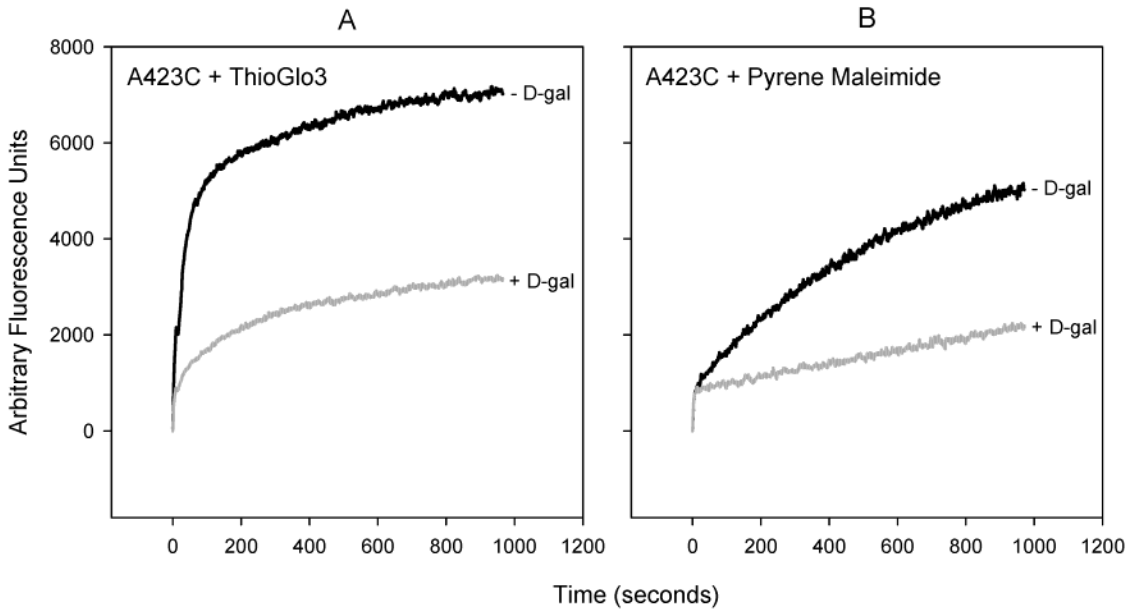

FIGURE 4: Effect of D-galactose on ThioGlo3 (A) and pyrene maleimide (B) labeling of Cys423 vSGLT proteoliposomes. In each experiment, the time course of the total fluorescence was recorded in 200 mM NaPi buffer at pH 7.0, in the presence and in the absence of 10 mM D-galactose.

mutants, since a 30-min preincubation of Cys423 proteoliposomes with 5 μM MIANS sharply reduced subsequent labeling with ThioGlo3. Cys423 was, however, fluorescently labeled by IAEDANS, the other anionic dye bearing the anilinonaphthalenesulfonate (ANS) moiety. The labeling time course was similar to that of pyrene maleimide. Also, the emission maximum blue-shifted from 496 nm (the cysteine adduct in Na^+ buffer) to 440 nm, suggesting that IAEDANS at Cys423 was in a hydrophobic protein pocket (*19*).

Ligand Effects. For one mutant, Cys423, the presence of D-galactose, but not L-glucose, in Na^+ diminished the rate of labeling with both ThioGlo3 and pyrene maleimide (Figure 4). D-Galactose had no effect during the labeling of Cys4, Cys80, Cys149, Cys228, or Cys546 with either ThioGlo3 or pyrene maleimide (not shown). There are two possible reasons for the effect of D-galactose on the rate of labeling of Cys423: (1) only a specific fraction of Cys423 proteins were alkylated in the presence of galactose, i.e., galactose in the presence of Na^+ blocked labeling; or (2) galactose induced a quench of the pyrene and Thioglo3 fluorescence.

Adding sugars in the presence of Na^+ after reaction of Cys423 with either the ThioGlo3 or pyrene maleimide assessed the possibility of a D-galactose-induced quench. Figure 5A shows that 10 mM D-galactose (and not L-glucose) did in fact quench the fluorescence of ThioGlo3-labeled Cys423 by ~40% in the presence of 200 mM Na^+. D-Galactose had no effect in the absence of Na^+. The D-galactose quench was concentration-dependent and saturable, and was half-maximal at 0.38 ± 0.03 mM (Figure 5B). A slight increase in fluorescence (<5%) was elicited by L-glucose. No such sugar quench was observed with the pyrene-labeled protein. These results demonstrate that the lower level of ThioGlo3 fluorescence observed for Cys423 in the presence of D-galactose relative to that in the absence of sugar (Figure 4A) is due, at least in part, to D-galactose quenching of the labeled protein.

D-Galactose had no effect on the steady-state fluorescence of any of the other five cysteine mutants labeled with ThioGlo3 and with pyrene maleimide. The small sugar-induced fluorescence increase seen with ThioGlo3-labeled Cys149 (Figure 5B) was nonspecific, as it could be elicited by either D-galactose or L-glucose. Finally, the sugars did not alter the emission spectra of either the ThioGlo3 or pyrene maleimide-labeled proteins.

The effect of D-galactose concentration on the steady-state fluorescence of ThioGlo3-labeled Cys423 was also determined at a Na^+ concentration approximating the $K_{0.5}$ (10 mM, Figure 5C). In this case, the half-maximal D-galactose concentration increased about 8-fold to 3 ± 1 mM, while there was little change in the maximum quench (judged by the small increase in the quench when the Na^+ was added to 200 mM in the presence of 100 mM D-galactose). The effect of Na^+ concentration on the D-galactose quench was examined at two different sugar concentrations (Figure 5D). At both D-galactose concentrations, the quench increased with increasing Na^+ concentration, but the maximum quench attainable in 0.5 mM D-galactose was lower than that in 20 mM D-galactose (20 vs 40%). Increasing the D-galactose concentration from 0.5 to 20 mM at 200 mM Na^+ increased the quench from 20 to 40% as anticipated. In addition, the Na^+ $K_{0.5}$ was 2-fold lower at 20 mM D-galactose than at 0.5 mM D-galactose (5 ± 1 vs 10 ± 3 mM).

Resonance Energy Transfer. The double-cysteine mutant Cys149/Cys423 was labeled with 15 μM pyrene maleimide in the presence and in the absence of Na^+, with and without 10 mM D-galactose. Tris(2-carboxyethyl)phosphine (TCEP) was added to 10 mM to ensure against disulfide formation. The emission spectrum (400−550 nm) was typical of the pyrene-labeled single-cysteine mutants and showed no evidence of pyrene excimer formation under any experimental condition.

Energy transfer between any vSGLT1 tryptophan (donor) and a ThioGlo3 (acceptor) tethered to vSGLT1 was explored with each single-cysteine mutant. Figure 6 shows an example of energy transfer from tryptophan(s) excited at 288 nm to a tethered ThioGlo3. Energy transfer was characterized by

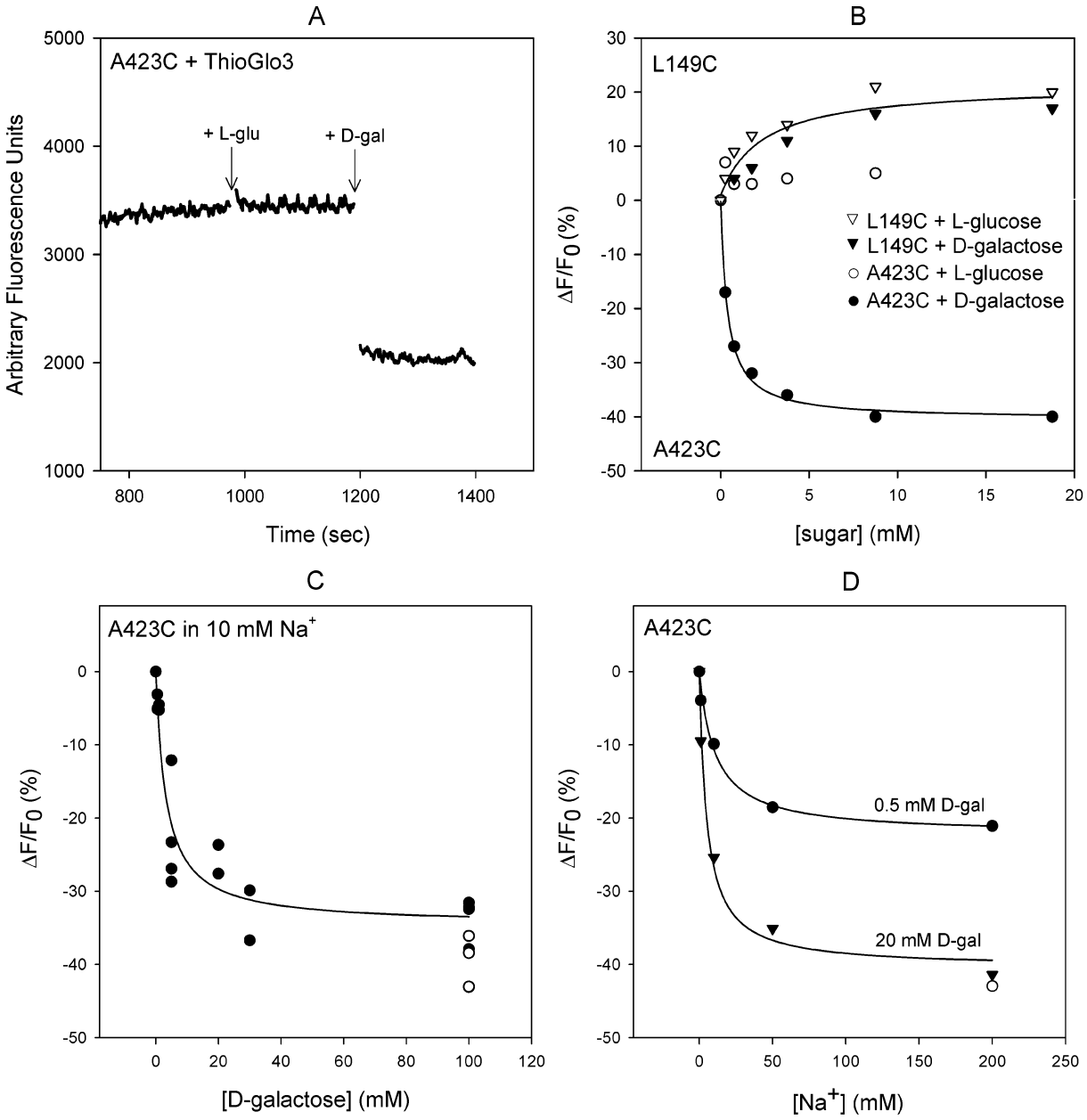

FIGURE 5: Effect of D-galactose and Na^+ on the fluorescence of ThioGlo3-labeled Cys423 vSGLT proteoliposomes. (A) Proteoliposomes were incubated in 200 mM NaPi buffer pH 7.0 for 800 s as described in Figure 3; 10 mM L-glucose and D-galactose were added to the cuvette at the time indicated. (B) The effect of increasing the D-galactose (and L-glucose) concentrations on the fluorescence of two ThioGlo3-labeled mutants. The experiments were carried out in 200 mM NaPi buffer as described in (A), but the final D-galactose (L-glucose) concentrations ranged from 0 to 20 mM. (C) The effect of increasing the D-galactose concentration (0−100 mM) on the fluorescence of ThioGlo3-labeled Cys423 at a reduced sodium concentration of 10 mM NaPi (●). After D-galactose had been added to 100 mM, the sodium concentration was increased to 200 mM (○). (D) The sodium concentration dependence of the D-galactose quench of ThioGlo3-labeled Cys423. Two experiments were carried out in 0.5 mM (●) and 20 mM (▼) D-galactose, where the sodium concentration was increased incrementally from 0 to 200 mM. At the end of the 0.5 mM D-galactose experiment, D-galactose was added to bring the sugar concentration to 20 mM (Open circle). All data are reported as the ligand-induced change in fluorescence (F/F_0, %). The apparent affinities ($K_{0.5}$) and maximum quenches ($\Delta F/F_{0max}$) were obtained by fitting the quench/concentration curves to the equation $F/F_0 = (\Delta F/F_{0max})\text{-}[S]/(K_{0.5} + [S])$ using the nonlinear fitting method in SigmaPlot (SPCC, Chicago, IL).

a reduction in the tryptophan emission intensity at 327 nm, with a concomitant increase in the ThioGlo3 emission intensity at 443 nm. (No emission at 443 nm was observed with the unlabeled protein.) Resonant energy transfer was also observed with ThioGlo3 derivatives of all but the Cys228 mutant, but ligands had no effect (data not shown).

DISCUSSION

Previous studies on the intrinsic tryptophan fluorescence, the ATR-FTIR spectrum, and H/D exchange have demonstrated that cotransported substrates produce conformational changes in vSGLT (*4*, *5*). Here, using cysteine-scanning and fluorescence probes, we set out to localize these substrate-induced conformational changes in the cotransporter. Of the cysteine mutations in seven of the eight external hydrophilic domains, only Cys423, located in the putative sugar-binding domain between TMHs 10 and 11, exhibited specific substrate effects on the rate and level of fluorescence labeling. D-Galactose elicits a quench of ThioGlo3 fluorescence at Cys423 in a Na^+-dependent, saturable fashion, while

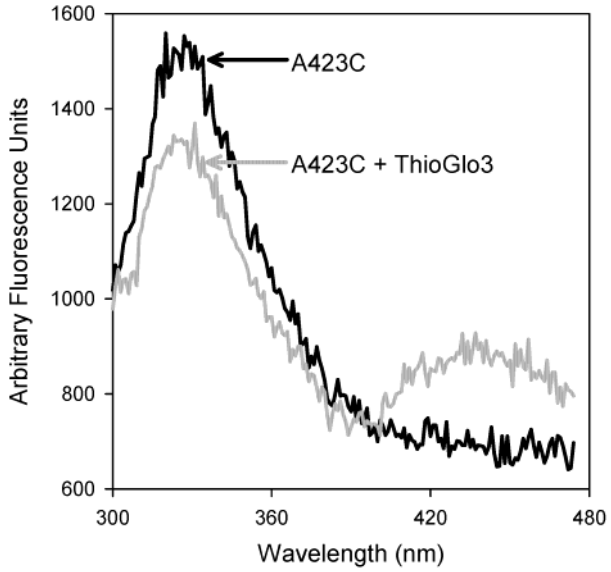

FIGURE 6: Energy transfer from vSGLT tryptophan donors to ThioGlo3. Cys423 vSGLT proteoliposomes were added to 200 mM KPi buffer, pH 7.0, and the emission spectra were taken from 300 to 480 nm after excitation at 288 nm. Next, 5 μM ThioGlo3 was added to the cuvette, and after 30 min the new spectra were recorded. Note the decrease in the vSGLT emission spectra after labeling of Cys423 with ThioGlo3, and the concomitant appearance of ThioGlo3 emission at 443 nm due to energy transfer from tryptophan.

the nontransported analogue L-glucose was without effect. From quench data, the apparent affinity for D-galactose ($K_{0.5}$ = 0.38 mM) was similar to values previously found for Na^+/galactose transport by vSGLT. The apparent affinities for transport were 0.2 mM in proteoliposomes (*3*) and 0.6 mM for the D-galactose increase in the intrinsic tryptophan fluorescence (*5*). These results suggest that conformational changes at or near the external hydrophilic loop between TMHs 10 and 11 are involved in Na^+-dependent D-galactose binding or transport.

This conclusion is supported by results showing that D-galactose in the presence of Na^+ slowed the reactions of both ThioGlo3 and pyrene maleimide with Cys423 (Figure 5). Neither D-galactose in the absence of Na^+ nor L-glucose in the presence or in the absence of Na^+ was able to mimic this effect. Furthermore, this Na^+/galactose effect was restricted to Cys423 and not evident at Cys4, Cys80, Cys149, Cys228, or Cys546. Previously we have shown that Na^+/sugar transport by Cys425, a cysteine on the same hydrophilic loop as Cys423, was blocked by MTSEA treatment in a Na^+/glucose protectable fashion (*6*).

The present results with vSGLT are also quite similar to those we obtained with the human SGLT1 mutant Q457C, in which Cys457 resides on the external domain homologous to that of *Vibrio* A423C (*9*, *10*). MTSEA and other alkylating reagents blocked Na^+/sugar transport by Q457C, yet no such inhibition was observed in the presence of Na^+ and transported sugars. Furthermore, transported sugars increased the fluorescence of Q457C, labeled with tetramethylrhodamine-6-maleimide (TMR6M), in the presence of Na^+. There is additional compelling evidence that Gln457 in this domain of human SGLT1 interacts with the glucose 1-carbon hydroxyl and the pyranose ring oxygen during binding and translocation through SGLT1 (*21*).

The kinetic effects of Na^+ and D-galactose on Cys423 ThioGlo3 fluorescence parallel those on the kinetics of SGLT1 Na^+/sugar transport (*7*, *8*). In both cases, increasing the Na^+ concentration resulted in an increase in the apparent affinity for sugar (decreases the $K_{0.5}$) and an increase in the maximum quench and the maximum rate of transport. In contrast, increasing the sugar concentration increased the apparent Na^+ affinity but did not change the maximum quench and rate of transport (see Figure 5B−D). Such kinetics are the hallmark of an ordered bireactant system where Na^+ binds first to increase the affinity of the protein for sugar (see ref *22*). One apparent difference between the bacterial and mammalian sugar transporters is the stoichometry of Na^+ to sugar transport, 1/1 vs 2/1, but this may be due to the fact that the quality of the Na^+ activation data for vSGLT (Figure 5D) does not permit an accurate estimate of a Hill coefficient. Nevertheless, the present results support a common mechanism for Na^+/sugar cotransport by the bacterial and human cotransporters.

One advantage of studies on vSGLT over hSGLT is that it is straightforward to carry out cysteine-scanning experiments on the bacterial transporter. There is only one native cysteine in vSGLT, and this can be removed so that cysteine-scanning experiments can be carried out against a Cys-less background. In the mammalian sugar transporters there are 12−16 cysteines, and mutation of one these in hSGLT1 (C292Y) eliminates trafficking of the transporter to the plasma membrane (*23*). Thus, it is impractical to carry out cysteine-scanning studies on a Cys-less background in mammalian transporters.

There are two effects of D-galactose on the fluorescence of Cys423 that are related to protein conformation, one on the accessibility of the residue to the probe and another on the microenvironment of the attached probe. D-Galactose reduced the rate of pyrene maleimide reaction with Cys423, inhibiting access possibly due to a Na^+-dependent change in conformation. D-Galactose also quenched bound ThioGlo3 by changing interactions between the probe and the protein and/or water. Galactose did not quench pyrene maleimide fluorescence, and this must reflect the differences in structure, shape, and polar groups of the fluorescence probes (see Figure 2) and differences in the microenvironment of the probes tethered to Cys423. It is reasonable to suggest that the naphthopyran, pyrene, and naphthyl rings and their substitutent groups have different rates of access to the Cys423 pocket on SGLT in the presence and in absence of ligands, and that once bound they have different exposures to both water and the residues lining the walls of the pocket. Another case is exemplified by the divergent effects of sugars on tetramethyl rhodamine 5 and 6 maleimides (TMR6M- and TMR5M) covalently bound to Cys457 and Cys454 in human SGLT1. At each location, sugars increase the TMR6M fluorescence yet the TMR5M fluorescence decreases (*10*; also Diez-Sampedro, A., Loo, D. D. F, and Hirayama, B. A., unpublished results). This suggests another approach to the micro-architecture of cotransporters based on the structure/activity relationships of fluorescent probes.

Energy transfer from ThioGlo3 to tryptophan was observed for all of the cysteine mutants except 228. It is reasonable to expect energy transfers from all 12 typtophans (Figure 1) to ThioGlo3 at each cysteine, since the Förster distance is ~18 Å (*24*) and the dimensions of vSGLT in the plane of

the membrane are ~50 Å × ~70 Å (*3*).

Support for the topology (Figure 1 and ref *2*) comes from the observation that both ThioGlo3 and pyrene maleimide reacted with all six cysteine mutants (Cys4, Cys80, Cys149, Cys228, Cys423, and Cys546) and that MTSEA and MTSES pretreatment blocks labeling, indicating that all six cysteine residues are readily accessible to the aqueous solution. The lack of reaction of the fluorescence probes with Cys477 is probably explained, at least in part, by the short length of the loop between helices 12 and 13 in vSGLT relative to the mammalian members of the family and steric inaccessibility. Additional supporting evidence for the topology of vSGLT includes (1) the fact that the N-terminal methionine is located on the extracellular side of the plasma membrane, as deduced from electrospray ionization mass spectrometry (*3*), and (2) experimental studies with other members of the SGLT gene family, e.g., the mammalian Na^+/iodide (NIS), human Na^+/glucose, and bacterial Na^+/proline (PutP) cotransporters (*2*, *25*, *26*).

In conclusion, the present study provides evidence that the global changes in the structure of the Na^+/galactose transporter reported in our previous ATR-FTIR study occur in the C-terminal half of the protein, at or near the hydrophilic domain connecting transmembrane helices 10 and 11. This fits with our thinking about the mechanism of sugar binding and translocation through the human SGLT1 and *lactose permease* symporters (*27*). What we have not yet learned from our studies of SGLT proteins is the location of the Na^+-induced structural change.

REFERENCES

1. Sarkar, R. I., Okabe, Y., Tsuda, M., and Tsuchiya, T. (1996) Sequence of a Na^+/glucose symporter gene and its flanking regions of *Vibrio parahaemolyticus*, *Biochim. Biophys. Acta 1281*, 1−4.
2. Turk, E., and Wright, E. M. (1997) Membrane Topological Motifs in the SGLT Cotransporter Family, *J. Membr. Biol. 159*, 1−20.
3. Turk, E., Kim, O., Le Court, J., Whitelegge, J. P., Eskandari, S., Lam, J. T., Kreman, M., Zampighi, G., Faull, K. F., and Wright, E. M. (2000) Molecular characterization of *Vibrio parahaemolyticus* vSGLT: a model for sodium-coupled sugar cotransporters, *J. Biol. Chem. 275*, 25711−25716.
4. le Coutre, J., Turk, E., Kaback, R. H., and Wright, E. M. (2002) Ligand-induced Differences in Secondary Structure of the *Vibrio parahaemolyticus* Na^+/Galactose Contransporter, *Biochemistry 41*, 8082−8086.
5. Veenstra, M., Turk, E., and Wright, E. M. (2002) A Ligand Dependent Conformational Change of the Na+/Galactose Cotransporter of *Vibrio Parahaemolyticus*, Monitored by Tryptophan Fluorescence, *J. Membr. Biol. 185*, 249−255.
6. Xie, Z., Turk, E., and Wright, E. M. (2000) Characterization of the *Vibrio parahaemolyticus* Na^+/glucose cotransporter: A bacterial member of the SGLT Family, *J. Biol. Chem. 275*, 25959−25964.
7. Parent, L., Supplisson, S., Loo, D. D. F., and Wright, E. M. (1992) Electrogenic properties of the cloned Na^+/glucose cotransporter: I. Voltage−Clamp studies, *J. Membr. Biol. 125*, 49−62.
8. Parent, L., Supplisson, S., Loo, D. D. F., and Wright, E. M. (1992) Electrogenic properties of the cloned Na^+/glucose cotransporter: Part II. A Transport model under non rapid equilibrium conditions, *J. Membr. Biol. 125*, 63−79.
9. Loo, D. D. F., Hirayama, B. A., Gallardo, E. M., Lam, J. T., Turk, E., and Wright, E. M. (1998) Conformational changes couple Na^+ and glucose transport, *Proc. Natl. Acad. Sci. U.S.A.. 95*, 7789−7794.
10. Meinild, A. K., Hirayama, B. A., Wright, E. M., and Loo, D. D. F. (2002) Fluorescence studies of ligand-induced conformational changes of the Na^+/glucose cotransporter, *Biochemistry 41*, 1250−1258.
11. Panayotova-Heiermann, M., Loo, D. D. F., Klong, C.-T, Lever, J. E., and Wright, E. M. (1996) Sugar binding to Na^+/glucose cotransporters is determined by the C-terminal half of the protein, *J. Biol. Chem. 271*, 10029−10034.
12. Panayotova-Heiermann, M., Eskandari, S., Zampighi, G. A., and Wright, E. M. (1997) Five transmembrane helices form the sugar pathway through the Na^+/glucose transporter, *J. Biol. Chem. 272*, 0324−20327.
13. Panayotova-Heiermann, M., Leung, D. W., Hirayama, B. A., and Wright, E. M. (1999) Purification and functional reconstitution of a truncated human Na^+/glucose cotransporter (SGLT1) expressed in *E. coli*, *FEBS Lett. 459*, 386−290.
14. Aiyar, A., and Leis, J. (1993) Modification of the megaprimer method of PCR mutagenesis: improved amplification of the final product, *Biotechniques 14*, 366−369.
15. Schägger, H., and von Jagow, G. (1987) Tricine−sodium dodecyl sulfate−polyacrylamide gel electrophoresis for the separation of proteins in the range from 1 to 100 kDa, *Anal. Biochem. 166*, 368−379.
16. Heukeshoven, J., and Dernick, R. (1985) Simplified method for silver staining of the proteins in polyacrylamide gels and the mechanism of silver staining, *Electrophoresis 6*, 103−112.
17. Heukeshoven, J., and Dernick, R. (1988) Improved silver procedure for fast staining in PhastSystem Development Unit. I. Staining of sodium dodecyl sulfate gels, *Electrophoresis 9*, 28−32.
18. Meinild, A. K., Loo, D. D. F., Hirayama, B. A., Gallardo, E. M., and Wright, E. M. (2001). Coupling between the Na^+ and sugar domains of the human Na^+/glucose cotransporter, *Biochemistry 40*, 1897−11904.
19. Haugland, R. P. (2002) *Handbook of Fluorescent Probes and Research Products*, 9th ed., Eugene, OR.
20. Langmuir, M. E., Yang, J.-R., Moussa, A. M., Laura, R., and LeCompte, K. A. (1995) New naphthopyranone based fluorescent thiol probes, *Tetrahedron Lett. 36*, 3989−3992.
21. Diez-Sampedro, A., Wright, E. M., and Hirayama, B. A. (2001) Residue 457 controls sugar binding and transport in the Na^+/glucose cotransporter, *J. Biol. Chem. 276*, 49188−49194.
22. Segel, I. W (1975) *Enzyme Kinetics*: *Behavior and Analysis of Rapid Equilibrium and steady-state enzyme systems*, John Wiley & Sons, New York.
23. Martín, M. G., Lostao, M. P. Turk, E., Lam, J., Kreman, M., and Wright, E. M. (1997) Compound missense mutations in the sodium/D-glucose cotransporter (SGLT1) results in trafficking defects, *Gastroenterology 112*, 1206−1212.
24. Lakowicz, J. R. (1999) *Principles of Fluorescence Spectroscopy*, Kluwer Academic Publishers, New York.
25. De La Vieja, A., Dohan, O., Levy, O., and Carrasco, N. (2001) Molecular analysis of the sodium/iodide symporter: Impact on thyroid and extrathyroid pathophysiology, *Physiol. Rev. 80*, 1083−1105.
26. Jung, H. (2002) He sodium/substrate symporter family: structural and functional features, *FEBS Lett. 529*, 73−77.
27. Abramson, J., Smirnova, I., Kasho, V., Verner, G., Kaback, H. R., and Iwata, S. (2003) Structure and Mechanism of the Lactose Permease of *Escherichia coli*, *Science 301*, 610−615.

BI0357210